Elsevier Editorial System(tm) for Food Chemistry

Manuscript Draft

Manuscript Number: FOODCHEM-D-16-04593R1

Title: Unravelling the nanostructure of strawberry fruit pectins by endo-polygalacturonase digestion and atomic force microscopy

Article Type: Research Article (max 7,500 words)

Keywords: Atomic force microscopy; cell wall; Fragaria × ananassa; homogalacturonan; pectins; rhamnogalacturonan; strawberry

Corresponding Author: Dr. Jose A. Mercado,

Corresponding Author's Institution: Universidad de Malaga

First Author: Candelas Paniagua

Order of Authors: Candelas Paniagua; Andrew R. Kirby; A. Patrick Gunning; Victor J Morris; Antonio J Matas; Miguel A. Quesada; Jose A. Mercado

Abstract: Pectins analysed by AFM are visualized as individual chains, branched or unbranched, and aggregates. To investigate the nature of these structures, sodium carbonate soluble pectins from strawberry fruits were digested with endo-Polygalacturonase M2 from Aspergillus aculeatus and visualized by AFM. A gradual decrease in the length of chains was observed as result of the treatment, reaching a minimum LN value of 22 nm. Branches were not visible after 2h of digestion. The size of complexes also diminished significantly with the enzymatic digestion. A treatment to hydrolyse rhamnogalacturonan II borate diester bonds neither affected chains length or branching nor complex size but reduced the density of aggregates. These results suggest that chains are formed by a mixture of homogalacturonan and more complex molecules composed by a homogalacturonan unit linked to an endo-PG resistant unit. Homogalacturonan is a structural component of the complexes and rhamnogalacturonan II could be involved in their formation

December 14, 2016

Dear Editor

Please, find enclosed the revised version of our ms no. FOODCHEM-D-16-04593 and our answers to the reviewer`s concerns. Main changes made in the manuscript are labelled in red.

Looking forward to hearing from you

Yours sincerely

José A. Mercado
Dep. Biología Vegetal
Universidad de Málaga
29071, Málaga, Spain

Comments to referees

First, we would like to thank both referees for their excellent comments and suggestions. Our answers to their concerns are described below. Main modifications made in the manuscript are labelled in red.

Reviewer 1

1) There are a lot or abbreviations used which makes this a difficult read, consider to use less?

The number of abbreviations have been reduced as suggested

2) I think the digested material needs to be analysed in some other way as well, such as size exclusion chromatography.

In this paper, we were interested in the effect of endo-PG digestion in the structure of linear strands and aggregates, and this could not be analysed by size exclusion chromatography. Additionally, the amount of material used in the AFM was insufficient to do this.

3) This paper clearly follows on from similar papers from the same group. And while the methods are referenced, more details are needed in this paper. For example, a comment about why butanol is used, and most importantly about how the AFM data has been analysed. How was Ln and Lw calculated? Plus show an example image of the features for each digestion time that was picked and measured – now the analysis is a black box!

Butanol is used to stop desorption of the molecules from the substrate and to allow imaging under liquid rather than in air. A comment on this has been included in the new version (p. 8, l. 198). LW and LM were calculated from the measured distribution functions using standard formula for the appropriate moments of the distribution function (Posé et al., 2012). The measured contour length is the length of the backbone plus the length of the attached branches. This was already indicated in the old version (p. 9, l. 206, old version). Example images of the different structures measured have been included in Supplementary Fig. 3.

4) The potential for errors need to be discussed, what checks have been made to ensure the contact mode is not destroying or moving the material on the surface? How long are images taken with the same tip – are there any tip deterioration effects? For the smallest features, have tip broadening effect been considered? Eventually you will just image the tip, which will skew your size/length data

The use of butanol and the selected normal force were chosen to minimise any distortion or disruption of the molecules. Successive images of the samples would reveal any displacement or damage to the sample. Tip deterioration normally arises due to absorption of material onto the tip – the conditions chosen minimise this and when it does occur it is evident in changes in successive images showing increased broadening, displacement or destruction of the molecules. Fresh tips used if deterioration observed. In general, the measured contour lengths are very much larger than the likely broadening knowing the tip radius and the width of the molecules from x-ray fibre diffraction data. If this were not so then there would be noticeable differences in the observed widths of the molecules, or parts of the molecules, when observed parallel to or perpendicular to the scan direction – this was not seen in the data. A comment on this has been included in the new version (p. 9, l. 203).

5) In general the quantitative and qualitative statements made (for example, 'level of branching was diminished after pectinase treatment') need to be clearly justified by examples in images

This would be difficult to show because the values are calculated for multiple scans of the sample and single images of individual molecules would not be representative.

6) The error signal images should also have a z-scale. Plus were the imaging done with a similar setpoint in all cases to give similar error images?

Fig. 1 and Supplementary Figs. 2 and 3 have been changed by the corresponding topographical images with the z-scale since topographical images were used for height measurements to identify individual molecules and branches and for calculations of the volume of the aggregates. Similar setpoints were used in all images.

7) The images have some noise, filtering may improve visibility

Figures have been improved by using the software Gwyddion

8) Page 14 line 345-346 Claim needs to be substantiated by pointing to data

Representative images of unbranched chains, branched chains and micellar aggregates have been included in the new version as indicated in the point 3.

9) Page 17 line 400 (data not shown) – with so little data already in this paper, I really think this data should be included or statement removed

The statement has been removed as suggested

10) In the discussion it is hard to follow what is own results, what is results from this paper and what is from literature. Be more explicit in the grammar and tenses used!

The discussion has been revised as suggested

11) Rha – abbreviation not explained

Rha abbreviation has been defined the first time that it was used (p. 4, l. 76)

12) Page 11 line 273 'data adjusted to' should be 'fitted to'

Corrected in the new version

13) Page 18 line 444 'tri-dimensional' should be 'three-dimensional'

Corrected in the new version

14) Nice afm paper to read and cite is Koziol, Cybulska et al Food Biophysics 2015

This paper has been cited (p. 5, l. 105)

15) Table 1: what is a, b, c etc in table?

These letters are used to differentiate median values statistically different. This was already defined in the old version

16) Table 1: relates to previous comment, but more info of how these values were extracted is needed

The statistical test employed was mentioned in the Table and more information was included in the M&M section "Statistical analysis"

17) Table 2: How was molecular weights measured??? If AFM, how was calculation done?

MWs were estimated with the volumes of the aggregates as described in M&M of the old version (p. 9, l. 222 new version)

18) Figure 1: Figure text is extremely long – be brief and put text in paper instead

Legend of Figure 1 has been shortened

19) AFM data could be displayed on better scale in general. Both the topography and the error signals…

Scale chosen to show representative sample – after degradation zooms could be shown but they would contain lesser numbers of molecules and would be less representative

Reviewer 2

There is valuable data presented in this manuscript but I believe the authors have overstated their results and not accurately reported content from some literature citations.

Thanks for the comment. We have modified the manuscript as suggested by the referee and we have included new references to support our results and hypothesis.

1. P1, l1 I do not believe the authors provide sufficient data to support this statement. I would suggest a different Title.

Title has been changed by "Unravelling the nanostructure of strawberry fruit pectins by endo-polygalacturonase digestion and atomic force microscopy"

2. P2. l30 This indicates the pectins had a relatively low DM or had a non-random distribution of charge in order for the EPGs to decrease MW. Was the DM of the pectin determined?

Pectins analysed in this study were demethylated since they were extracted with sodium carbonate, an alkaline extraction that breaks ester linkages. See FT-IR profiles of sodium carbonate strawberry pectins in Posé et al. (2012) (Carbohyd. Polym. 88:882-890; Fig. 1)

3. P2, l32 EPG cuts 1-4 linkages, what was the linkage for the branch, and what were the sugars?

Previous studies indicated that branches present in linear chains were formed by galacturonic acid since they were much more longer than neutral sugars side chains and the removal of neutral sugars by acid hydrolysis did not affect pectin structure (Round et al., 1997, Carbohyd. Res. 303:251-253; Round et al., 2001, Carbohyd. Res. 331:337-342; Round et al., 2010, Carbohyd. Res. 345: 487-497). The nature of the branch linkage to the backbone is unknown, but Round et al. (2010) suggested that it involved only galacturonic acid. This has been clarified in the new version (page 5, line 113; p.14, l.343). Our results support the homogalacturonan nature of these long branches.

4. P2, l35 complex, not complexes

Corrected in the new version

5. P2, l37 RG I or a stretch of esterified GalAs

In our study, we suggest that the endo-PG resistant unit could be RGI but further studies are needed to confirm this hypothesis. Thus, we prefer to maintain the term "endo-PG resistant unit" in the Abstract. On the other hand, a stretch of esterified GalAs is discarded since sodium carbonate pectins are de-esterified, as commented in point 2.

6. P2, l38 this abbreviation should be defined at first use

RGII has been defined as suggested

7. P3, l53 the audience might first be told that pectin is largely composed of galacturonic acid

This comment has been included in the first sentence of the introduction (p. 2, l. 50).

8. P4, l88 Coenen et al, Carbohydrate Polymers 70 (2007) 224-235 should be included here and their refutation should be disclosed.

Results of Coenen et al. (2007) supporting the HG-RGI alternating pectin model have been included as suggested (p. 4, l. 89)

9. P4, l90 an RGI core

Corrected in the new version

10. P5, l10 I believe it is also necessary to bring into this entire discussion the works of Fishman et al J. Agric. Food Chem. 2008, 56, 1471-1478

A comment about the results obtained by Fishman et al. (2008) has been included (p. 5, l. 117).

11. P5, l103 can it differentiate between various types of bonds or describe the nature of the branch point?

AFM cannot provide information about the nature of bonds in branch points. To avoid misinterpretation, this sentence has been changed in the new version as follow: "AFM has provided new information on the branching of the pectin backbone; features such as contour length, branch length and distribution can be studied through this technology" (p.5, l. 106).

12. P5, l105 Round et al. 2010 (there is no 2011 listed in the bibliography)

Corrected in the new version

13. P5. l107 how does it differentiate between a branch and a side chain?

In this study, the terms "*branch*" and "*sidechains*" have been used as synonymous. The sentence has been changed to avoid confusion (p.5, l. 111).

14. P6, l132 dissociates

Corrected in the new version

15. P7, l168 why are there no spaces between the number and the unit throughout the manuscript?

This has been modified in the new version

16. *P8, l179 should be a raised dot (1 mg·ml-1*)

Corrected in the new version

17. P9, l202 Pose et al 2012 stated (p884, Sec 2.4)

The length of single pectin chains was determined by plotting the main chain with the freehand tool of the software. To determine the chain lengths, individual molecules were defined as strands that were not entangled with, or overlapping other strands, that were long enough to be exactly visualized, and which lay entirely within the scanned area (Adams, Kroon, Williamson, & Morris, 2003).

and

Furthermore, other features were also characterized, including the number of branch points and branch lengths. This indicates they did not include branches as part of the contour length.

In this paper, as well as in Posé et al. (2012), contour length corresponds to total polymer length, including backbone and branches. This is defined in the M&M section (p. 9, l. 218)

18. P9, l213 How were the areas of the images chosen for measurements determined? Was it a random choice based on a grid pattern?

It wasn't a random choice; the choice of regions are the ones that provide the best clarity to enable accurate measurement of discrete polymers in contrast to aggregated chains which cannot be measured separately.

19. P10, l234 dilution, 1:105 (enzyme/water? or 1 x 10 e5?)
Correspond to $1:10^5$ (enzyme:water). This has been clarified in the new version (p.10, l. 249)

20. P10, l239 please point out representative examples on the Fig. 2.
P10, l240-241 and point these out
Zoomed images of strands and aggregates have been included in Supplementary Fig. 3

21. P10, l243 "In general…" please provide some data to support this.Was there a statistical difference?
Contour length data are shown in Table 1. The statistical analysis of control and transgenic samples has been included in the new Table 1 (ME data, capital letter). This sentence has been deleted and a comment about the size of control and transgenic strands before digestion has been included in the new version, p. 11, l. 275.

22. P11, l252 statistically significant?
No statistical analysis has been performed since strands and aggregates almost disappeared after 4 h of enzymatic treatment, as can be clearly observed in Fig. 2.

23. P11, l256 error bars on Fig.3 please
Supplementary Fig. 3 (renamed as Supplementary Fig. 4 in the new version) represents the relative frequency of data at every length category. No error bars can be displayed in this representation.

24. P11, l258 10 - 400 nm with 50 and 75 nm being
Corrected in the new version

25. *P12, l286 pectinase is commonly used to describe a cocktail of pectin hydrolysing and depolymerising enzymes. There was no mention of pectinase treatment in the M&M.*
Reviewer is right. The term "pectinase" has been changed by "endo-PG".

26. P12, l289 the common belief is that EPG needs a minimum of four consecutive deesterified GalA units to hydrolyse a GalA-GalA bond. Are you implying that these branches points contain this composition? (Chen and Mort, 1996, Carbohydrate Polymers 29. 129-136)
As the branches disappeared with the treatment, we suggest that branches are mainly composed of GalA, as previously postulated by other authors (see previous comments).

27. P12, l292 This was for 'aggregates', not for individual chains. Assuming 0.4 nm per GalA and an average length of 100 nm we would have 250 GalA units at 176 daltons each = 44,000 daltons = 44 kDa. But you are reporting MWn of between 1000 and 3000 kDa. Would you explain this please.
Data on Table 2 correspond to MW of aggregates, not to individual chains. These MW were calculated with the volume of the aggregates, as described in M&M, section 2.6. The MW of the individual strands can be calculated from the estimated number of residues provided in the manuscript (p. 16, l. 383, new version) yielding values close to those indicated by the referee.

28. P13, l302 what exactly constitutes an 'aggregate'? Is it definable?

Aggregates are pectin complexes distinguishable in AFM by height measurements. As commented in the manuscript, it has been postulated that these complexes are supramolecular pectin structures present in cell walls (Round et al., 2010).

29. P13, l322 please provide refs for "previous investigations"
References have been included in the new version (p. 14, l. 336).

30. P14, l325 are these sugars considered part of the pectic 'backbone'?
Arabinose and galactose are sidechains of RGI. The term “backbone” has been deleted from this sentence (p. 14, l. 337, new version).

31. P14, l329 "neutral sugars" so, they are not part of the pectin backbone
Correct

32. P14, l331 what about Coenen et al 2007?
Coenen et al. (2007) analysed pectin oligomers by chromatographic techniques obtained after acid hydrolysis. In this part of the discussion, we mentioned those studies that analysed the structure of pectins during acid hydrolysis by AFM. Anyway, the results obtained by Round et al. (2010) are compatible with those derived from Coenen et al. (2007), since, according to these authors, aggregates would be composed of HG and RGI.

33. P14, l338 is there any other place rha could be coming from? Any thoughts on why rha is susceptible in one vs. the other?
As commented in the paper, different rhamnose composition and/or a different pectin structure that could make Rha residues more susceptible could explain these contrasting results.

34. P14, l344 is there any compositional or linkage data in the literature that might shed light on what these branches might be?
These long pectin branches have been observed by AFM in pectins from different sources, as cited in the paper. As the frequency of ramification is quite low, the number of linkages that would be necessary to form these branches would be too low and rather difficult to detect by linkage analysis. However, some linkage analyses (Talmadge et al., 1973, Plant Physiol. 51: 158-173; McNeil et al., 1980, Plant Physiol 66:1128-1134; Peña and Carpita, 2004, Plant Physiol. 135, 1305-1313) showed evidences of minor amounts of 2,4- and 3,4-linked galacturonosyl residues which could represent branch points. A comment on this has been included in the new version (p. 15, l. 367).

35. *P14, l349 not really random, see Benen et al Eur. J. Biochem. 259, 577-585*
The word “randomly” has been deleted (p. 15, l. 362)

36. P15, l350-351 Senechal simply cites Verlent (2005) and Ferrari on this assertion. Verlent makes no mention of the number of contiguous GalAs required for EPG hydrolysis only stating that EPG is more active on pectin that has been deesterified by a blockwise PME. Ferrari makes no mention of the initiation site required for EPG cleavage. On the other hand, as previously noted Chen and Mort suggested a binding site with a minimum of four GalAs for EPG cleavage based on experimental data.
Perhaps I overlooked some mention of the binding site for EPG in the Senechal, Verlent or Ferrari papers. If there indeed was no mention of an experimental basis for the assertion that a minimum binding site was composed of two deesterified GalAs I am concerned about why the Senechal reference was included and how a misinterpretation may affect the conclusions reached in this manuscript.

We cited Senechal et al. (2015) because this is one of the most recent review about the mode of action of pectinases. As discussed by the referee, Senechal et al. (2015) also stated that plant endo-PG prefers HG with more than four demethylesterified residues. The sentence has been modified to indicate that endo-PG cleavage bonds in HG with at least four demethylesterified GalA and the study of Chen and Mort (1996) has been cited (p. 15, l. 362). In any case, this does not modify our conclusions because sodium carbonate pectins are deesterified, as discussed in point 2.

37. P15, l353 Are you saying the branches are HGs branched off of HGs? If that is your hypothesis please provide data to support or refute it. EPG hydrolyses a GalA 1-4 bond. Is there any data that it might hydrolyse a GalA 1-2, 1-3 or GalA GalA ester link through C6?

We have found that the length of individual strands and the percentage of branched strands diminished with the endo-PG treatment, suggesting that both structures are formed mainly by HG. This does not necessarily imply that endo-PG would hydrolyse other GalA-GalA bonds different to 1-4. Endo-PG could liberate small GalA oligomers containing the branch point, not visible by AFM.

38. P15, l354 This reference simply states that a commercial enzyme solution was used for "depectinization". Most likely a cocktail of pectinolytic hydrolases and does not support the GalA nature of branches.

Correct. This sentence has been deleted in the new version

39. P15, l359 why did you not try other enzymes to degrade these structures, i.e. pectin lyase. It would have been easy to confirm or refute the hypothesis that these remnants were HG.

We have tried a commercial rhamnogalaturonase, but the optimal conditions for AFM visualization of these samples have not been optimised yet.

40. *P16, l379 by EPG but other pectic enzymes were not tested.*

This sentence has been changed to "…resistant to endo-PG digestion" (p.16, l.389, new version)

41. P16, l381-382 according to B.M. Yapo et al. / Carbohydrate Polymers 69 (2007) 426-435, on p 433, last sentence before the Discussion, it is stated:
"leading to number- and weight-average degrees of polymerisation of 34-40 [GalA-Rha] disaccharide repeating units, in good agreement with previous reports on citrus pectin".
This does not agree with the estimate of 70-80 provided here.

In the manuscript, we indicated that the number of total residues in RGI was in the range 70-80. These values correspond to 34-40 disaccharide repeating units, as indicated by the referee. This sentence has been clarified in the new version as follow: "According to Yapo et al. (2007), RGI isolated backbone is about 70-80 residues, corresponding to 34-40 GalA-Rha disaccharide repeating units" (p. 16, l. 394).

42. P16, l389 these authors also pointed out that this conflicted with literature reports on MW.

As indicated by the referee, Coenen et al. (2007) stated in their conclusions that "*This hypothesis does, however, not account for the Mw of pectins (50–100 kDa), considering that the RGI element is 12 kDa and the HG element is 17.5 kDa (Prade, Zhan, Ayoubi, & Mort, 1999; Yapo et al., 2007; Zhan et al., 1998)*". However, none of the cited references provided the range of MW indicated by these authors (50-100 kDa). Therefore, it is not possible to know if that range of MW pectins corresponds to bulk pectins or specific pectin fractions. Moreover,

pectin size varied greatly with the source and the extraction procedure. Additionally, that statement contradicts their own data. Coenen et al. (2007) showed that the main peak in chromatographic profiles of untreated apple pectins had a MW between 10-35 KDa (Fig. 1, profile A), which was in accordance with their suggestion of pectin composed of one HG (17.5kDa) and one RGI (12 kDa) structural elements. As indicated by Anderson (J. Exp. Bot., 2016, 67: 495-502), the precise size distribution for most pectins remains poorly defined although the degree of polymerization of some pectin domains have been found to be fairly homogeneous. The chromatographic analysis of bulk pectins monitors the volume of the molecules in a complex mixture, based on hydrodynamic behaviour of polymers through a porous gel matrix. Long branched pectins and pectin aggregates, as depicted by AFM, could develop a more 'bulky' pectin mixture leading to an overestimation of pectin size. Furthermore, in agreement with Coenen et al. (2007) and results shown in this manuscript, Zhan et al. (1998) found that the analysis of endo-PG digestion of citrus pectins suggested that these pectins were composed of a HG region not interrupted by Rha, accounting for 80% of the starting material, and a RGI region with neutral side chains. This reference has been included in the discussion in the new version (p. 16, l. 397).

43. P16, l391 pectin lengths
Corrected in the new version

44. P16, l392 does not
Corrected in the new version

45. P16, l396 how much xylose was in the sample, was compositional analysis done?
Compositional analysis of strawberry sodium carbonate pectins has been shown in Posé et al. (2015), Carbohyd. Polym. 132:134-145. The proportion of Xyl was around 2.5 (mol % of neutral sugars)

46. P16, l396-397 the MW range listed does not agree with the dp listed, 20 kDa will not be 29 residues
This has been corrected as follows: "Xylogalacturonans are not degraded by endo-PGs. Molecular weights of 20-30 kDa and a backbone minimum degree of polymerization of 29-119 residues have been reported for XGA polymers (Yapo, 2011)" (p. 17, l. 413).

47. P17, l414 "strongly support" how so?
The number of complexes as well as their estimated MW diminished with the endo-PG digestion, suggesting that they are partly composed of HG. The word "strongly" has been removed and the paragraph has been rewritten for clarification (p. 17, l. 422).

48. P18, l440-441 what percentage were gone?
More than 80%. This has been included in the text (p. 19, l. 455).

49. P19, l454 consistent with what?
The expression "highly consistent" has been changed by "a reliable result" (p. 19, l. 467).

50. P19, l456 refs?
Correspond to the results showed in this paper. This sentence has been modified for clarification (p. 19, l. 467).

51. P19, l459-461 In their conclusion Coenen et al argued that it was unlikely that a pectin molecule contained only one HG and one RGI segment.
See our previous comments to point 42

52. P19, l468-473 I do not believe the data presented, nor the references cited are sufficient to support this hypothesis.

We don't agree with the referee. Our results are in agreement, among others, with those obtained by Round et al. (2010) and Zhang et al. (2014) using AFM, the MW of HG and RGI domains obtained by chromatographic analyses (Yapo et al., 2007; Yapo, 2011), the linkage analyses performed by Coenen et al. (2007) and the results of citrus pectin digested with endo-PG obtained by Zhan et al. (1998). The exact structure of pectins is largely unknown despite the numerous efforts that have been performed in their characterization for a long time. In this study, we propose a model that could explain the characteristics of the pectin structures observed by AFM in strawberry and many other fruits, but obviously, further research using AFM and other techniques are needed to validate this model.

Highlights:

1. Strawberry fruit pectins are visualized by AFM as linear chains and large complexes

2. Digestion with fungal endoPG reduces the size of linear chains and complexes

3. An acid treatment to eliminate RGII dimers diminishes the number of complexes

4. Pectin chains are formed by a mixture of HG and HG linked to an endoPG resistant unit

5. RGII dimers are involved in the formation of the pectin complexes

Unravelling the nanostructure of strawberry fruit pectins by endo-polygalacturonase digestion and atomic force microscopy

Candelas Paniagua [a], Andrew R. Kirby [b], A. Patrick Gunning [b], Victor J. Morris[b], Antonio J. Matas[a], Miguel A. Quesada [c], José A. Mercado[a*]

[a]Instituto de Hortofruticultura Subtropical y Mediterránea "La Mayora" (IHSM-UMA-CSIC), Departamento de Biología Vegetal, Universidad de Málaga, 29071, Málaga, Spain.

[b] Institute of Food Research, Norwich Research Park, Colney, Norwich, NR4 7UA, UK.

[c]Departamento de Biología Vegetal, Universidad de Málaga, 29071, Málaga, Spain.

*Corresponding author.

E-mail: mercado@uma.es (Jose A. Mercado)

Corresponding author:

José A. Mercado

Instituto de Hortofruticultura Subtropical y Mediterránea "La Mayora" (IHSM-UMA-CSIC), Dept. de Biología Vegetal, Universidad de Málaga, 29071, Málaga, Spain

e-mail: mercado@uma.es

Fax: +34 952 13 20 00

Abstract

Pectins analysed by AFM are visualized as individual chains, branched or unbranched, and aggregates. To investigate the nature of these structures, sodium carbonate soluble pectins from strawberry fruits were digested with endo-Polygalacturonase M2 from *Aspergillus aculeatus* and visualized by AFM. A gradual decrease in the length of chains was observed as result of the treatment, reaching a minimum L_N value of 22 nm. The branches were not visible after 2 h of enzymatic incubation. The size of complexes also diminished significantly with the enzymatic digestion. A treatment to hydrolyse rhamnogalacturonan II borate diester bonds neither affected chains length or branching nor complex size but reduced the density of aggregates. These results suggest that chains are formed by a mixture of homogalacturonan and more complex molecules composed by a homogalacturonan unit linked to an endo-PG resistant unit. Homogalacturonan is a structural component of the complexes and rhamnogalacturonan II could be involved in their formation.

Keywords: Atomic force microscopy, cell wall, *Fragaria* × *ananassa*, homogalacturonan, pectins, rhamnogalacturonan, strawberry

Abbreviations: AFM, atomic force microscopy; APEL, antisense pectate lyase plants; APG, antisense polygalacturonase plants; HG, homogalacturonan; L_N, number-average contour length; L_W, weight-average contour length; PDI, polydispersity index; PG, polygalacturonase; PL, pectate lyase; RG, rhamnogalacturonan; XGA, xylogalacturonan.

1. Introduction

Pectins, polymers largely composed of galacturonic acid (GalA), are one of the major components of plant cell walls and probably the most complex structural polysaccharide in nature (Vincken et al., 2003). Polyuronides influence the physical and mechanical properties of the primary cell wall, fulfilling important biological functions during cell growth and development (Bacic, Harris & Stone, 1988; Bidhendi & Geitmann, 2016; Peaucelle et al., 2011). The middle lamellae between primary cell walls are also enriched in pectin, where it functions in regulating intercellular adhesion (Willats, McCartney, Mackie & Knox, 2001). Moreover, pectins have potential applications in areas such as the food industry and medicine, as a source of fibres and anticarcinogenesis products (Glinsky & Raz, 2009; Maxwell, Belshaw, Waldron & Morris, 2012).

Homogalacturonan (HG), a homopolymer of α-(1-4)-D-GalA which can be methylesterified at C-6 or acetylated at O-2 or O-3 is the most abundant polyuronide, accounting for 50-90% of most extracted pectins (Yapo, 2011). Rhamnogalacturonan II (RGII), xylogalacturonan (XGA) and other minority polymers, such as apiogalacturonan, galactogalacturonan and arabinogalacturonan, are often referred as substituted galacturonans due to the presence of a common galacturonan backbone (Ridley, O'Neill & Mohen, 2001; Yapo, 2011). RGII is composed of nine galacturonyl residues, containing clusters of four heteropolymeric side chains with more than 20 uncommon sugar residues and 20 different glycosidic linkages (O'Neill, Ishii, Albersheim & Darvill, 2004). RGII can dimerize by means of borate ester links, being dimeric Rhamnogalacturonan II the predominant form *in muro* (Yapo, 2011). XGA is a linear HG partially substituted at O-3 positions with single residues of xylose and/or small, 2-8 residues, β-D-Xyl side chains. XGAs are frequently found in storage tissues of reproductive organs (Yapo, 2011). Finally, rhamnogalacturonan I (RGI) polymers

76 are highly ramified pectins having a backbone of the repeating disaccharide [→2)-α-L-
77 Rhap-(1→4)-α-D-GalpA-(1→], partly substituted at O-4 or O-3 positions of rhamnose
78 (Rha) residues by arabinan, galactan and arabinogalactan side chains (Willats et al.,
79 2001; Yapo, 2011).

80 Although the chemical composition of pectins is well known, the way in which
81 these domains are inter-connected within the cell wall is unclear. Fig. 1 shows the
82 alternative models for pectin assembly that have been proposed. The most accepted
83 model shows the pectin composite as a linear backbone composed by HG (smooth
84 regions), that can be interspersed with rhamnosyl residues, alternated at regular
85 intervals with branched RGI, XGA, arabinan and arabinogalactan (hairy regions) (De
86 Vries, Rombouts, Voragen & Pilnik, 1982; Yapo, 2011) (Fig. 1A). The number of
87 residues in both regions varied in the range 75-120 for HG domains and 70-80 for RGI.
88 An alternative model postulates that RGI is the main pectin backbone, and linear HG
89 and XGA would be side chains of the RGI core (Vincken et al., 2003) (Fig. 1B). The
90 analysis of the oligomers obtained after acid hydrolysis of apple pectins performed by
91 Coenen, Bakx, Verhoef, Schols & Voragen (2007) partly supported the De Vries et al.
92 (1982) model, although the model where HG is positioned as a RGI side chain could
93 not be excluded. More recently, Yapo (2011) suggested a different model, in which the
94 pectin complex is formed by an RGI core, decorated with neutral sugars and XGA
95 side chains, connected with two unbranched HG blocks at the extremes (Fig. 1C).

96 Many methodological approaches from different scientific disciplines have been
97 used to characterize pectic polysaccharides. Pectins are complex heterogeneous
98 molecules and microscopic techniques, which can visualise individual molecules, are
99 ideal for characterizing such populations. Both transmission electron microscopy and
100 atomic force microscopy (AFM) provide suitable resolution and have been used to

study pectin molecules. AFM offers the advantages of imaging the molecules in a liquid environment and of providing direct information on the height of the molecules: the latter being particularly useful for ensuring single molecules are being studied and allowing branching of the molecule backbone to be distinguished from overlapping of molecules where the height would double at the crossover point (Kirby, Gunning & Morris, 1996; Round, Rigby, MacDougall, Ring & Morris, 2001; Koziol, Cybulska, Pieczywek & Zdunek, 2015). AFM has provided new information on the branching of the pectin backbone; features such as contour length, branch length and distribution can be studied through this technology (Round et al., 2001; Round, Rigby, MacDougall & Morris, 2010; Morris, Gromer, Kirby, Bongaerts & Gunning, 2011). In general, AFM studies of fruit pectins, independently of the species, show individual polymers, unbranched or with a reduced number of long branches, which can be connected to make up large fibres or micellar aggregates (Posé et al., 2012; Round et al., 2001; Yang, Chen, An & Lai, 2009; Zareie, Gokmen & Javadipour, 2003). It has been postulated that branches in linear chains are composed by HG, while neutral sugar are present as much shorter chains, not detected by AFM (Round et al., 2001; Round et al., 2010). The aggregates could represent or be remains of supramolecular pectin structures present *in muro*. Along this line, Fishman, Chau, Cooke & Hotchkiss (2008) observed strands and spherical particles integrated into networks in microwave-extracted pectins isolated from sugar beet pulp. Pectin polymer lengths and the number of aggregates diminish as the fruit ripen or during the postharvest storage (Paniagua et al., 2014). More recently, Posé et al. (2015) used AFM to analyse pectins isolated from strawberry fruits with a pecate lyase (PL) or a polygalacturonase (PG) gene downregulated by antisense transformation, and they found a close relationship between nanostructural complexity of polyuronides and fruit texture.

AFM has also provided new information on the nature of aggregated structures present in pectin extracts from the cell wall. In sodium carbonate soluble pectins from unripe tomato, Round, Rigby, MacDougall & Morris (2010) found that the release of neutral sugars by acid hydrolysis of the samples with 0.1 M HCl at 80ºC at different incubation times, did not affect individual pectin lengths but decreased the size of aggregates. These authors suggested that pectin aggregates were a mixture of RGI and HG, while isolated chains were composed of polygalacturonic acid. By contrast, Zhang, Cui, Xiao & Wang (2014), using a similar approach, observed a decrease in the length of individual pectin chains after acid hydrolysis of *C. edulis* and citrus peel, suggesting that these polymers contain RGI.

This study uses AFM to investigate further the structures of pectin samples from ripe native and mutant strawberry fruit. To this purpose, initially, we have analysed the effect of fungal endo-PG digestion in chain contour length and the number and size of aggregates in sodium carbonate soluble pectins from control and transgenic fruits with a PL or a PG gene downregulated. In addition, we used AFM to analyse pectins subjected to mild acid hydrolysis at 25ºC, a treatment that dissociates dimeric RGII complex into monomeric RGII (Kobayashi, Matoh & Azuma, 1996), to elucidate the role of RGII in the formation of the micellar aggregates.

2. Materials and methods

2.1. Plant material

Ripe strawberry (*Fragaria* × *ananassa*, Duch., cv. 'Chandler') fruits from control, non-transformed, plants and transgenic plants carrying antisense sequences of a pectate lyase gene, *FaplC* (line APEL39, described in Santiago-Doménech et al. (2008)), or a

polygalacturonase gene, *FaPG1* (line APG29, described in Posé et al. (2013)) were used as the source of pectins. Transgenic ripe fruits showed a strong reduction in *FaplC* or *FaPG1* mRNA levels, higher than 95% in both genotypes.

2.2. Cell wall isolation and pectin extraction

The procedure used for the isolation of the cell wall material from ripe strawberry fruits was based on the protocol of Redgwell, Melton & Brasch (1992) as modified by Santiago-Doménech et al. (2008). Briefly, 10-15 frozen fruits were ground to a powder in liquid N_2 and 20 g were homogenised in 40 ml of PAW (phenol: acetic acid: water, 2:1:1, w:v:v). The homogenate was centrifuged at 4000 *g* for 15 min and the supernatant filtered through Miracloth (Merck, Bioscience, UK). After centrifugation, the pellet obtained was treated with 90% aqueous DMSO to solubilise the starch. The extract was then centrifuged at 4000 *g* and the pellet washed twice with distilled water. The water fraction was discarded, and the de-starched pellet, which is considered the cell wall material, was lyophilised.

The cell wall material was fractionated as described previously (Santiago-Doménech et al., 2008) to obtain the Na_2CO_3 soluble pectin fraction. Briefly, cell wall material was washed overnight with deionised water, centrifuged at 6000 *g* for 15 min and the pellet was sequentially extracted with 0.05 M trans-1,2-diaminocyclohexane-N,N,N'N'-tetraacetic acid (CDTA) in 0.05 M sodium acetate buffer, pH 6, followed by 0.1 M Na_2CO_3 containing 0.1% $NaBH_4$. Sodium carbonate soluble fraction was exhaustively dialysed against distilled water and stored at -20ºC, as aqueous solution, until analysed by AFM. Galacturonic acid was determined by the carbazole method (Filisetti-Cozzi & Carpita, 1991), using galacturonic acid as standard.

176

177 *2.3. Endo Polygalacturonase digestion*

178 Pectin samples diluted to a concentration of 0.5 mg·ml^{-1} of GalA in 0.1 mM
179 ammonium bicarbonate buffer, pH 5.5, were digested with a diluted endo-PG (280
180 U/mg; E.C. 3.2.1.15; from *Aspergillus aculeatus*; Megazyme) at 40ºC (optimum
181 enzyme temperature recommended by the manufacturer). Enzymatic digestions were
182 stopped at 0, 1, 1.5, 2, 4, 6, 8 and 24 h by boiling the samples for 10 min. Different
183 dilutions of endo-PG were tested to avoid artefacts and interferences in the AFM
184 images. Samples incubated with buffer without enzyme were used as control. After
185 digestion, samples were visualized by AFM as described in the following sections.

186

187 *2.4. Acid hydrolysis treatment*

188 To determine the effect of dimeric RGII removal on pectin nanostucture, samples were
189 subjected to mild acid hydrolysis following the procedure of Kobayashi et al. (1996).
190 Samples (1 mg·ml^{-1}) were incubated in 0.1M HCl for 30 min at RT, neutralized with 1 N
191 NaOH and dialysed against pure water for 2 h. Then, samples were processed for AFM
192 visualization as described later. Non-treated samples and pectin samples treated with
193 water instead of 0.1 M HCl were used as controls.

194

195 *2.5. Atomic force microscopy*

196 AFM samples were prepared as described by Posé et al. (2012). Pectin samples were
197 diluted in water to a concentration of 2-4 µg·ml^{-1}. Then, 3 µl were pipetted onto freshly-
198 cleaved mica and dried over a heating block at 37 ºC. The sample was then inserted into
199 the liquid cell of the AFM microscope (manufactured by ECS, East Coast Scientific,
200 Cambridge, UK) and visualized under re-distilled butanol. Butanol was used as an

imaging solvent to limit desorption of the molecules from the substrate and to eliminate capillary condensation effects (Kirby et al., 1996; Round et al., 2001). Silicon nitride cantilevers for contact mode (Budget Sensors, Bulgaria) were used with a quoted force constant of 0.2 $N \cdot m^{-1}$. Samples, 1 μm^2 area, were scanned in contact mode at a frequency of 2 Hz. The use of butanol and the selected normal force minimise any distortion or disruption of the molecule. Fresh tips were used if deterioration observed. No noticeable differences in the widths of the molecules, or part of the molecules, were seen when observed parallel to or perpendicular to the scan direction, indicating a minor tip broadening effect. Images were collected and stored in both topographical and error signal mode. Topographical images were used for height measurements to identify individual molecules and branches and for calculations of the volume of the aggregates. The calibration of the AFM microscope was assessed with the calibration standard TGZ02 (NT-MDT Co. Building 167, Zelenograd, Moscow, 124460, Russia).

2.6. AFM image analysis

AFM files were converted to TIFF files using Paint Shop Pro v. 5.00 software and analysed offline. Individual molecules were defined as strands that were not entangled with, or overlapping other strands, and ones that lay entirely within the scanned area (Adams, Kroon, Williamson & Morris, 2003). Contour length of individual strands, defined as total length including backbone and branches, was analysed by plotting the length of the chains with the freehand tool of ImageJ software (Posé et al., 2012). The number-average (L_N) and the weight-average (L_W) contour lengths and their ratio (L_W/L_N) or polydispersity index (PDI) were calculated as described previously (Posé et al., 2012). The volumes of pectin aggregates were estimated using the image analysis software Gwyddion (2.40win32). The software estimates the volume between grain

surface and the basis surface formed by Laplacian interpolation of surrounding values. The molecular weights of the aggregates were calculated from these volumes using a galacturonic molecular weight of 176 Da, representing each monomer as a cylinder of 0.435 nm in length and 0.4 nm in radius, as described by Round et al. (2010). The number of aggregates per μm^2 was also recorded. Ten to 20 images per treatment were taken and 200-300 individual measurements from independent images were obtained to represent contour length distributions and to perform statistical analysis.

2.7. Statistical analysis

All experiments were performed by triplicate. The GraphPad Prism software (v.5.0 b) was used for statistical analyses. The medians from the original length distributions were compared by non-parametric Kruskal–Wallis test. Differences in the branching of the polymer chains, presence/absence of branches, were analysed by Chi-square test. The number of aggregates per μm^2 of sample was analysed by Mann Whitney U test. All statistical tests were performed at $P = 0.05$.

3. RESULTS

3.1. Effect of polygalacturonase digestion on nanostructure of sodium carbonate pectin samples

In this experiment, pectin samples were digested with fungal endo-PG during different times, and visualized by AFM. Initially, several endo-PG concentrations were tested to ensure that the final conditions chosen did not lead to artefacts due to the presence of the enzyme or the buffer used in the studies: a low enzyme

dilution, 1:10^5 (enzyme:water) corresponding to 0.13 U·mg^{-1} GalA in the assay, was found to not interfere with AFM images on the pectin extracts. Representative topographical AFM images of samples from Control fruits before and after enzymatic incubations are shown in Fig. 2, and those corresponding to APG and APEL samples in Supplementary Figs. 1 and 2, respectively. AFM images of pectin samples before treatment showed isolated chains, unbranched or with a small number of long branches, independently of the genotype. Additionally, larger tri-dimensional structures or micellar aggregates were also visible at lower frequency. These structures were characterized by entangled pectins in the centre with emerging chains, some of which were similar in size to isolated pectic chains. Images of the different structures visualized by AFM can be shown in Supplementary Fig. 3.

As a result of endo-PG treatment, a gradual decrease in the main backbone length of isolated chains as well as in the length of their branches was observed in the three samples. This was especially evident after 4h of endo-PG digestion (Fig. 2; Supplementary Figs. 1, 2 and 3). After this time, the number of linear chains that could be observed in the samples decreased significantly. Similarly, the number of micellar aggregates and their size decreased with the time of digestion. After 24 h of treatment, AFM images showed few filamentous structures and aggregates, independently of the genotype.

Supplementary Fig. 4 shows the contour length distributions of isolated pectic chains from the three genotypes at different digestion times. Pectin length varied in the range 10-400 nm with 50 and 75 nm being the more abundant contour length classes in the three genotypes before treatment. Endo-PG digestion shifted sample distributions to shorter chain length, with most polymers in the 0-25 nm class after 24h of digestion. The contour length distribution parameters number-average (L_N),

276 weight-average (L_W) and the polydispersity index (PDI) are shown in Table 1. The
277 medians (ME) of the original data were also included and used for statistical
278 comparison. Before enzymatic treatment, isolated chains from transgenic samples
279 were significantly larger than those present in controls. In all the samples, the
280 median of the length distributions decreased with the endo-PG incubation time, with
281 the differences in the initial ME values statistically significant after 1.5 h of digestion
282 in the case of Control and APG samples or 2 h in the case of APEL pectins. After 24 h
283 of enzymatic treatment, the three samples showed similar contour length parameters
284 despite APG and APEL chains being significantly larger than control chains before
285 digestion. The minimum polymer chain length reached after 24 h digestion was
286 around 22 nm. PDI index remained unchanged during the whole digestion process,
287 consistent with a process of random single depolymerisation events (Round et al.,
288 2010).

289 L_N data were fitted to an exponential decay curve using the equation

$$L_N = L_{N0} + a.e^{-bx}$$

290 being L_{N0} the minimum polymer chain length, a the difference between the maximum
291 L_N value and L_{N0}, and b a rate constant, expressed in units of h^{-1}, that indicates how
292 rapidly the curve descends. The three samples fitted well to this equation with R^2
293 values close to or higher than 0.9 (Fig. 3). As expected, a values were higher in
294 samples from both transgenic lines when compared with control pectins; however, L_{N0}
295 values were similar in the three samples. Interestingly, APEL pectins showed a lower
296 rate constant than the rest of genotypes. The half digestion time, calculated as $0.692/b$,
297 yielded values of 1.68, 1.65 and 2.47 h for control, APG and APEL samples,
298 respectively.

299 The percentage of branched polymer chains before PG treatment was around 6%

300 in control and APEL samples and significantly higher, >30%, in APG, as previously
301 described by Posé et al. (2015) (Supplementary Fig. 5). The level of branching
302 diminished after endo-PG treatment, and after 2 h of treatment no branched pectic
303 chains were observed in Control and APG samples (Supplementary Fig. 5). However,
304 APEL samples still maintained a low percentage of branched chains, which
305 disappeared after 4h of endo-PG digestion (Supplementary Fig. 5).

306 The volumes of the complexes were estimated according to Round et al. (2010)
307 and used to calculate number-average and weight-average molecular weights before
308 and after 24 h of endo-PG digestion (Table 2). Before digestion, Control and APEL
309 samples showed complexes of similar molecular weights and slightly higher than
310 those observed in APG samples; however, the medians of the distributions were not
311 statistically different. After PG digestion, size of complexes diminished significantly,
312 reaching similar values in the three sample pectins (Table 2).

313

314 *3.2. Effect of mild acid treatment on pectin structure*

315 To investigate the role of RGII in the nano-structure of linear chains and aggregates,
316 pectin samples from APG fruits were subjected to a mild acid hydrolysis treatment,
317 0.1M HCl for 30 min at room temperature, to split dimmers of RGII. APG samples
318 were used because their pectins displayed the highest number of aggregates. Fig. 4
319 shows a representative image of pectins prior to and after mild acid hydrolysis.
320 Apparently, the length of isolated pectic chains was unaffected, as well as the size of
321 aggregates. However, the number of aggregates that appeared in the AFM samples
322 was notably reduced, from a mean value of 6 complexes/μm^2 before hydrolysis to 1
323 complex/μm^2 after hydrolysis.

324 Isolated polymer chains were measured before and after acid hydrolysis and their

basic parameters calculated (Supplementary Table 1). Although L_N and L_W values decreased slightly after acid treatment, the medians of the length chain distributions were not statistically different. Similarly, the length of the branches as well as the percentage of branched molecules was not affected by the acid hydrolysis treatment (results not shown). The M_N and M_W molecular weights of the aggregates that remained in the AFM samples after the hydrolysis treatment were similar to those observed in non-treated samples (Supplementary Table 1).

4. DISCUSSION

4.1 Isolated chains and branches visualized by AFM are mainly formed by galacturonic acid

Mild acid hydrolysis (0.1M HCl, 80ºC) of pectins at different times in combination with AFM has been used in previous investigations to determine the structure of polyuronides and the association among HG and RGI in native cell walls (Round et al., 2010; Zhang et al., 2014). This treatment cleaves glycosidic linkages at different rates, i.e. arabinose and galactose are released very rapidly, followed by rhamnose with galacturonic acid being the most resistant (Thibault, Renard, Axelos, Roger & Crépeau, 1993). After 72 h hydrolysis, almost pure HG was recovered in the acid-insoluble fraction (Thibault et al., 1993). Round et al. (2010) found that the loss of neutral sugars during the hydrolysis of carbonate pectins extracted from unripe tomato did not have a significant effect either on pectin chain or branch length (Round et al., 2010), suggesting that isolated chains, including long branches, were formed solely by HG and not interrupted by RGI. According to these authors, RGI was located mainly in the micellar aggregates, since the size of these structures decreased during acid

hydrolysis. By contrast, Zhang et al. (2014) observed a reduction of lengths of main backbone and branch in alkali-soluble pectins from rhizomes of *Canna edulis* and citrus peel after hydrolysis, indicating that Rha was located at the backbone chain. These contrasting results could be related to a different composition and/or structure of the pectins analysed, as demonstrated by the amount of Rha that remained in the samples after 72h of hydrolysis, 66% of the initial Rha in *C. edulis* vs. traces of Rha in tomato pectins (Round et al., 2010; Zhang et al., 2014).

A different strategy to unravel the structure of fruit pectins has been followed in this study consisting in the analysis of samples by AFM after digestion with a fungal endo-PG at different times. Undigested strawberry ripe fruit pectins appeared mainly as linear chains, unbranched or with a low number of branches, and as micellar aggregates. The structure of these aggregates frequently includes strands emerging from the central core with sizes that are similar to those of isolated chains. Similar linear chains and aggregates have previously been described in pectin samples extracted from other fruits, e.g. tomato, peach, jujuba and apricot (Chen et al., 2013; Round et al., 2001; Wang et al., 2012; Yang et al., 2009). Endo-PGs catalyse the hydrolytic cleavage of α-(1-4) bonds between at least four de-methylesterified GalA residues of the HG backbone (Chen and Mort, 1996; Sénéchal, Wattier, Rustérucci & Pelloux, 2015). The digestion of strawberry pectins with fungal endo-PG reduced pectin chain length and eliminated pectin branches. Our results strongly support a galacturonic acid nature of linear strands and branches. The nature of the linkage involving GalA branches is unknown but several linkage analyses have found minor amounts of 2,4- and 3,4-linked galacturonosyl residues (Talmadge, Keegstra, Bauer & Albersheim, 1973; McNeil, Darvill & Albersheim, 1980; Peña & Carpita, 2004), which could represent branch points of the main pectin chain.

In spite of the large decrease in pectin backbone length due to endo-PG digestion, the pectin backbone was not totally degraded by the enzyme. In the three samples analysed, linear chains reached their minimum length after 8h of endo-PG treatment and no further reduction was observed at 24 h of treatment. Interestingly, the average size of the strands that remained at the end of the experiment, about 22 nm, was similar in the three genotypes despite the higher initial size of APG or APEL chains. The number of carbohydrate residues as well as molecular mass of the pectic structures visualized by AFM can be estimated from L_N values considering a 3_1 helical structure with a pitch of 1.34 nm, data obtained from fibre diffraction analysis of polygalacturonic acid by Walkinshaw & Arnott (1981). According to this approach, the degrees of polymerization of strawberry carbonate pectins before endo-PG digestion were 164, 215 and 205 for Control, APG and APEL fruits. The number of residues in the remaining chains after 24 h of endo-PG treatment was estimated around 52 residues, independently of the genotype. It has been proposed that essentially pure HG contains approximately 72-117 residues (Thibault et al., 1993; Yapo, 2011; Yapo, Lerouge, Thibault & Ralet, 2007). Interestingly, the number of residues digested by endo-PG fits within this range, 112 residues in the control genotype, suggesting that isolated polymers visualized by AFM are formed by a pure HG domain linked to a shorter polymer resistant to endo-PG digestion. In the transgenic genotypes, the silencing of the genes encoding pectinolitic enzymes could protect pectins from degradation in vivo, yielding chains of longer size.

As a first hypothesis, the endo-PG resistant fraction of the linear chains observed in this study might correspond to RGI. According to Yapo et al. (2007), RGI isolated backbone is about 70-80 residues, corresponding to 34-40 GalA-Rha disaccharide repeating units. This value is slightly higher than the number of residues found in the

strawberry polymers remaining after endo-PG treatment. Zhan, Janssen & Mort (1998) observed that the digestion of commercial citrus pectins with endo-PG produced two fractions: a predominant region of uninterrupted 1,4-linked GalA residues, accounting for 80% by weight of the starting material, and a RGI region containing neutral side chains. In this respect, the analysis of the oligomer fragments released by acid hydrolysis of apple pectins indicated that both HG and XGA were covalently linked to RGI, with RGI at the reducing end of the oligomer and HG/XGA at the non-reducing end (Coenen et al., 2007). Interestingly, the absence of oligomers with HG at the reducing-end suggested that the backbone of apple pectin consisted of only one HG and one RGI structural element (Coenen et al., 2007). The putative presence of RGI residues in the backbone of strawberry pectin chains is supported by the observed reduction of pectin lengths after acid hydrolysis in *C. edulis* and citrus (Zhang et al., 2014). However, this hypothesis does not match with the results of Round et al. (2010) who found that chain length of tomato pectins was not altered after 24h of acid hydrolysis despite the amount of Rha being almost totally depleted. As an alternative explanation, the indigestible oligomer of the strawberry strands could correspond to XGA. Xylogalacturonans are not degraded by endo-PGs. Molecular weights of 20-30 kDa and a backbone minimum degree of polymerization of 29-119 residues have been reported for XGA polymers (Yapo, 2011). However, Posé et al. (2015) showed that the amount of xylose in strawberry pectins extracted with sodium carbonate is half the amount of Rha. Further experiments are needed to clarify this point. A hypothetical model for strawberry pectins based on the results obtained in this research is shown in Fig. 1D.

4.2 Aggregate complexes are partially degraded by fungal endo-PG and might be

stabilized by dimeric RGII

Round et al. (2010) found that the acid hydrolysis of tomato pectins reduced size of aggregated complexes observed in the AFM samples from 965 to 453 kDa, suggesting that complexes contained RGI, HG chains and irreducible aggregates of HG. In our case, the number-average MW (M_N) of the complexes observed in the strawberry samples was in the range 900-1700 kDa, a value slightly higher than the one observed by Round et al. (2010) in tomato. After 24 h of endo-PG digestion, the number of complexes decreased as well as their MW, reaching a mean M_N value of 654 kDa. These results support the hypothesis of the complexes being partly composed of HG.

On the other hand, untreated samples from down-regulated *FaPG1* fruits showed a higher amount of aggregates than control and APEL samples, although their size were slightly lower. This result indicates that plant polygalacturonases may be involved in the disassembly of the tridimensional structure of these aggregates during fruit ripening. The smaller size of APG aggregates could explain the higher rate constant of endo-PG digestion of APG linear chains obtained in the kinetic plots when compared with APEL pectins. Linear chains from both APEL and APG samples were larger than control, and therefore a lower digestion rate constant, higher half digestion time, would be expected. This occurred for APEL samples but not for APG pectins. As the complexes are degraded simultaneously to the linear chains, new shorter chains might be liberated from the smaller APG complexes during the initial stages of endo-PG digestion and this would account for the lower half digestion time of these pectins when compared with APEL samples.

Despite RGII being a minor pectin component in the cell wall, it is believed that it could play an important role in the regulation of the pore size and other physical properties of the cell wall (O'Neill et al., 2004). In the traditional pectin model of

alternating “smooth” and “hairy” regions, RGII is integrated in the HG backbone. In the alternative pectin model proposed by Vincken et al. (2003), RGII domains are included in HG domains which are covalently cross-linked to RGI. Additionally, RGII can cross-link by borate-diol ester two HG domains (Vincken et al., 2003). Yapo (2011) proposed that the formation of RGII dimers is a prerequisite for pectin macromolecular formation. This molecule is able to form dimers via borate diester bridges between RGII molecules belonging to two different layers of pectins and also between pectic molecules within the same layer. Kobayashi et al. (1996) suggested the use of mild acid hydrolysis at room temperature for a short time (30 min) to break borate ester cross-linking without altering glycosidic linkages. The use of this treatment in strawberry pectins diminished in an 80% the number of aggregates, without altering the length of isolated chains or the branch pattern. Moreover, the volume of the aggregates that remain after treatment did not change. These results indicate that dimeric RGII could be a key component of micellar aggregates and part of their three-dimensional structure.

5. CONCLUSIONS

The enzymatic treatment of sodium carbonate soluble pectins from strawberry fruits with fungal endo-PG decreased the length of pectin chains and the number of branches. However, these single molecules were not completely degraded and a minimum pectin length of 22 nm, corresponding to about 52 residues, was reached after 8 h of digestion. It is noteworthy that the size of the chain that was degraded is in good agreement with the size of pure HG obtained by different methods (Morris, Ralet, Bonnin, Thibault & Harding, 2010; Thibault et al., 1993; Yapo et al., 2007). The existence of an endo-PG resistant unit as structural component of the linear chains was a reliable result, i.e. the results shown in the present study indicate that pectins from transgenic fruits with

pectinase genes silenced were significantly larger than control but the endo-PG digestion of these samples also yielded polymers of around 22 nm. These results suggest that linear polymers observed by AFM are a mixture of HG and more complex molecules composed of a HG unit linked to a different polymer, likely RGI although the nature of this component is speculative. On the other hand, the pectin complexes observed in AFM samples were partially degraded by endo-PG treatment, indicating that these structures also contain HG, as suggested by Round et al. (2010). Contrary to endo-PG treatment, hydrolysis with diluted HCl at room temperature did not modify the length of pectin strands, but significantly diminished the presence of aggregates. This treatment breaks borate diester bonds between RGII, and therefore, our results indicate that RGII has a key role in the formation and/or stabilization of these complexes. Based on these results, a new hypothetical model for strawberry pectin assembly is proposed (Fig. 1D) in which the pectin chains are formed by HG, unbranched or with a low number of HG branches, and more complex molecules formed by a single HG unit linked to a RGI unit. RGII would be located in the HG backbone or HG branches allowing the formation of pectin aggregates through borate diester bridges between adjacent RGII from different pectin molecules.

Acknowledgements: This work was supported by the Ministerio de Economía y Competitividad of Spain and FEDER EU Funds (grant references AGL2011-24814 and AGL2014-55784-C2-1-R) and by a Ramón y Cajal project RYC-2011-08839 awarded to AJM. The use of AFM was supported by the Biotechnology and Biological Science Research Council (BBSRC) through its core strategic grant to IFR.

References

Adams, E. L., Kroon, P. A., Williamson, G., & Morris, V. J. (2003). Characterisation of heterogeneous arabinoxylans by direct imaging of individual molecules by atomic force microscopy. *Carbohydrate Research*, *338*, 771-780.

Bacic, A,, Harris, P. J., & Stone, B. A. (1988). Structure and function of plant cell walls. In J. Preiss J (Ed.), *The Biochemistry of Plants*, (pp. 297–371). New York: Academic Press.

Bidhendi, A. J., & Geitmann, A. (2016). Relating the mechanics of the primary plant cell wall to morphogenesis. *Journal of Experimental Botany*, *67*, 449-461.

Coenen, G. J., Bakx, E. J., Verhoef, R. P., Schols, H. A., & Voragen, A. G. J. (2007). Identification of the connecting linkage between homo- or xylogalacturonan and rhamnogalacturonan type I. *Carbohydrate Polymers*, *70*, 224-235.

Chen, E. M. W., & Mort, J. A. (1996). Nature of sites hydrolyzable by endopolygalacturonase in partially-esterified homogalacturonans. *Carbohydrate Polymers, 29*, 129-136.

Chen, Y., Chen, F., Lai, S, Yang, H., Liu, H., Liu, K., Bu, G., & Deng, Y. (2013). In vitro study of the interaction between pectinase and chelate-soluble pectin in postharvest apricot fruits. *European Food Research and Technology, 217*, 1438-2377.

De Vries, J. A., Rombouts, F. M., Voragen, A. G. J., & Pilnik, W. (1982). Enzymic degra- dation of apple pectins. *Carbohydrate Polymers*, *2*, 25-33.

Filisetti-Cozzi, T. M. C. C., & Carpita, N. C. (1991). Measurement of Uranic Acids without interference from neutral sugars. *Analytical Biochemistry, 197*,157-162.

Fishman, M. L., Chau, H. K., Cooke, P. H., & Hotchkiss Jr., A. T. (2008). Global structure of microwave-assisted flash-extracted sugar beet pectin. *Journal of Agricultural and Food Chemistry, 56*, 1471-1478.

Glinsky, V. V., & Raz, A. (2009). Modified citrus pectin anti-metastatic properties: one

525 bullet, multiple targets. *Carbohydrate Research, 344*, 1788-1791.
526 Kirby, A. R., Gunning, A. P., & Morris, V.J. (1996). Imaging polysaccharides by
527 atomic force microscopy. *Biopolymers, 38*, 355-366.
528 Kobayashi, M., Matoh, T., & Azuma, J. (1996). Two chains of rhamnogalacturonan II
529 are cross-linked by borate-diol ester bonds in higher plant cell walls. *Plant*
530 *Physiology*, *110*, 1017-1020.
531 Koziol, A., Cybulska, J., Pieczywek, P. M., & Zdunek, A. (2015). Evaluation of
532 structure and assembly of xyloglucan from tamarind seed (*Tamarindus indica* L.)
533 with atomic force microscopy. *Food Biophysics, 10*, 396-402.
534 Maxwell, E. G., Belshaw, N. J., Waldron, K. W., & Morris, V. J. (2012). Pectin: An
535 emerging new bioactive food polysaccharide. *Trends in Food Science and*
536 *Technology*, *24*, 64-73.
537 McNeil, M., Darvill, A. G., & Albersheim, P. (1980) Structure of plant cell walls. X.
538 Rhamnogalacturonan I, structurally complex pectic polysaccharide in the walls of
539 suspension-cultured sycamore cells. *Plant Physiology, 66*, 1128-11234.
540 Morris, G. A., Ralet, M. -C., Bonnin, E., Thibault, J. -F., & Harding, S. E. (2010)
541 Physical characterization of the rhamnogalacturonan and homogalacturonan
542 fractions of sugar beet (*Beta vulgaris*) pectin. *Carbohydrate Polymers*, *82*, 1161-
543 1167.
544 Morris, V J. Gromer, A, Kirby, A. R, Bongaerts, R. J. M. & Gunning, A. P. (2011) Using
545 AFM and force spectroscopy to determine pectin structure and (bio) functionality
546 *Food Hydrocolloids, 25*, 230-23.
547 O'Neill, M. A., Ishii, T., Albersheim, P., & Darvill, A.G. (2004). Rhamnogalacturonan
548 II: structure and function of a borate cross-linked cell wall pectic polysaccharide.
549 *Annual Review of Plant Biology, 55*,109-139

550 Paniagua, C., Posé, S., Morris, V. J., Kirby, A. R., Quesada, M. A., & Mercado, J. A.
551 (2014). Fruit softening and pectin disassembly: an overview of nanostructural pectin
552 modifications assessed by atomic force microscopy. *Annals of Botany, 114*, 1375-
553 1383.
554 Peaucelle, A., Braybrook, S. A., Le Guillou, L., Bron, E., Kuhlemeier, C., & Höfte, H.
555 (2011). Pectin-induced changes in cell wall mechanics underlie organ initiation in
556 *Arabidopsis*. *Current Biology*, *21*, 1720-1726.
557 Peña, M. J., & Carpita, N. C. (2004). Loss of highly branched arabinans and
558 debranching of rhamnogalacturonan I accompany loss of firm texture and cell
559 separation during prolonged storage of apple. *Plant Physiology*, *135*, 1305-1313.
560 Posé, S., Kirby, A. R., Mercado, J. A., Morris, V. J., & Quesada, M. A. (2012).
561 Structural characterization of cell wall pectin fractions in ripe strawberry fruits
562 using AFM. *Carbohydrate Polymers*, *88*, 882-890.
563 Posé, S., Paniagua, C., Cifuentes, M., Blanco-Portales, R., Quesada, M. A., &
564 Mercado, J. A. (2013). Insights into the effects of polygalacturonase *FaPG1* gene
565 silencing on pectin matrix disassembly, enhanced tissue integrity, and firmness in
566 ripe strawberry fruits. *Journal of Experimental Botany*, *64*, 3803-3815.
567 Posé, S., Kirby, A. R., Paniagua, C., Waldron, K. W., Morris, V. J., Quesada, M. A., &
568 Mercado, J. A. (2015). The nanostructural characterization of strawberry pectins
569 in pectate lyase or polygalacturonase silenced fruits elucidates their role in
570 softening. *Carbohydrate Polymers*, *132*, 134-145.
571 Redgwell, R. J., Melton, L. D., & Brasch, D.J. (1992), Cell wall dissolution in
572 ripening kiwifruit (*Actinidia deliciosa*): solubilization of the pectic polymers.
573 *Plant Physiology*, *98*,71–81.
574 Ridley, B. L., O'Neill, M. A., & Mohnen, D. (2001). Pectins: Structure, biosynthesis,

and oligogalacturonide-related signaling. *Phytochemistry, 57*, 929-967.

Round, A. N., Rigby, N. M., MacDougall, A. J., Ring, S. G., & Morris, J. V. (2001). Investigating the nature of branching in pectin by atomic force microscopy and carbohydrate analysis. *Carbohydrate Research*, *331*, 337-342.

Round, A. N., Rigby, N. M., MacDougall, A. J., & Morris, V. J. (2010). A new view of pectin structure revealed by acid hydrolysis and atomic force microscopy. *Carbohydrate Research*, *345*,487-497.

Santiago-Doménech, N., Jiménez-Bemúdez, S., Matas, A. J., Rose, J. K. C., Muñoz-Blanco, J., Mercado, J. A., & Quesada, M. A. (2008). Antisense inhibition of a pectate lyase gene supports a role for pectin depolymerization in strawberry fruit softening. *Journal of Experimental Botany*, *59*, 2769-2779.

Sénéchal, F., Wattier, C., Rustérucci, C., & Pelloux, J. (2014), Homogalacturonan modifying enzymes: structure, expression, and roles in plants. *Journal of Experimental Botany*, *65*, 5125-5160.

Talmadge, K. W., Keegstra, K., Bauer, W. D. & Albersheim, P. (1973) The structure of plant cell walls. I. The macromolecular components of the walls of suspension-cultured sycamore cells with a detailed analysis of the pectin polysaccharides. *Plant Physiology, 51*, 158-173.

Thibault, J. -F., Renard, C. M. G. C., Axelos, M. A. V., Roger, P., & Crépeau, M.-J. (1993). Studies of the length of homogalacturonic regions in pectins by acid hydrolysis. *Carbohydrate Research*, *238*, 271-286.

Vincken, J., Schols, H. A., Oomen, R. J. F. J., McCann, M. C., Ulvskov, P., Voragen, A. G. J., & Visser, R. G. F. (2003). If homogalacturonan were a side chain of Rhamnogalacturonan I. Implications for cell wall architecture. *Plant Physiology, 132*, 1781-1789.

600 Walkinshaw, M. D., & Arnott, S. (1981). Conformations and interactions of pectins. I.
601 X-ray diffraction analyses of sodium pectate in neutral and acidified forms. *Journal*
602 *of Molecular Biology*, *153*, 1055-1074.
603 Wang, H., Chen, F., Yang, H., Chen, Y., Zhang, L., & An, H. (2012). Effects of
604 ripening stage and cultivar on physicochemical properties and pectin
605 nanostructure of jujubes. *Carbohydrate Polymers*, *89*, 1180-1188.
606 Willats, W. G. T., McCartney, L., Mackie, W., & Knox, J. P. (2001). Pectin: cell
607 biology and prospects for functional analysis. *Plant Molecular Biology*, *47*, 9-27.
608 Yang, H., Chen, F., An, H., & Lai, S. (2009). Comparative studies on nanostructures of
609 three kinds of pectins in two peach cultivars using atomic force microscopy.
610 *Postharvest Biology and Technology, 51*,391-398.
611 Yapo, B. M. (2011). Pectic substances: from simple pectic polysaccharides to complex
612 pectins - A new hypothetical model. *Carbohydrate Polymers*, *86*, 373-385.
613 Yapo, B. M., Lerouge, P., Thibault, J. -F., & Ralet, M. -C. (2007). Pectins from citrus
614 peel cell walls contain homogalacturonans homogeneous with respect to molar
615 mass, rhamnogalacturonan I and rhamnogalacturonan II. *Carbohydrate Polymers*,
616 *69*, 426-435.
617 Zareie, M. H., Gokmen, V., & Javadipour, I. (2003). Investigating network, branching,
618 gelation and enzymatic degradation in pectin by atomic force microscopy. *Journal*
619 *of Food Science and Technology*, *40*, 169-172.
620 Zhang, J., Cui, J, Xiao, L., & Wang, Z. (2014). The combination of atomic force
621 microscopy and sugar analysis to evaluate alkali-soluble *Canna edulis* Ker pectin.
622 *Food Chemistry*, *156*, 64-71
623

624 **Table 1.** Descriptors of contour length distributions of sodium carbonate soluble
625 pectins extracted from ripe strawberry fruits from control, APG and APEL lines at
626 different times of digestion with endo-PG. L_N: number-average, L_W: weight-average,
627 PDI: L_W/L_N ratio, ME: median values of the original data. ME values with different
628 letters are significantly different by non-parametric Kruskal–Wallis test at P=0.05.
629 Capital letters for comparison among genotypes in columns and lower letters for
630 comparison among the different digestion times within each genotype.

		Digestion time (hours)							
		0	1	1.5	2	4	6	8	24
Control	L_N (nm)	73.2	65.3	46.6	40.8	33.7	28.9	20.2	25.2
	L_W (nm)	88.3	86.9	61.2	50.0	49.4	38.2	30.2	33.1
	PDI	1.2	1.3	1.3	1.2	1.5	1.3	1.5	1.3
	ME (nm)	64.6Ba	55.0Ca	39.1Cb	35.6Bb	29.3Bc	27.1Bc	20.2Bd	24.4Acd
APG	L_N (nm)	95.9	78.5	63.4	37.9	49.4	32.4	19.1	22.4
	L_W (nm)	126.1	96.5	87.0	48.5	68.3	45.3	25.4	30.1
	PDI	1.3	1.2	1.4	1.3	1.4	1.4	1.3	1.3
	ME (nm)	81.7Aa	71.1Bab	57.4Bbc	31.4Cd	41.9Acd	28.5Bde	22.9Bf	23.4Aef
APEL	L_N (nm)	91.4	87.9	78.0	54.9	39.2	38.4	33.8	22.9
	L_W (nm)	120.3	106.9	101.5	65.3	55.3	50.7	44.4	30.8
	PDI	1.3	1.2	1.3	1.2	1.4	1.3	1.3	1.3
	ME (nm)	81.7Aa	82.2Aa	72.6Aab	51.7Ab	33.4Bc	33.4Ac	31.0Acd	22.4Ad

631

632

633 **Table 2.** Molecular weights of aggregates from control, APG and APEL pectin
634 samples after digestion with endo-PG. M_N: number-average, M_W: weight-average,
635 PDI: ratio M_W/M_N, ME: median values of the original data. ME values with different
636 letters are significantly different by non-parametric Kruskal–Wallis test at P=0.05.
637 Capital letters for comparison among genotypes in columns and lower letters for
638 comparison between 0 and 24 hours within each genotype.

Aggregates		Digestion time (hours)	
		0	24
Control	M_N (kDa)	1690.3	618.7
	M_W (kDa)	2727.8	886.4
	PDI	1.6	1.4
	ME (kDa)	1406.4Aa	503.8Ab
APG	M_N (kDa)	1170.0	703.1
	Mw (kDa)	1396.1	1223.3
	PDI	1.2	1.7
	ME (kDa)	960.0Aa	571.4Ab
APEL	M_N (kDa)	1755.0	641.7
	Mw (kDa)	2863.8	928.8
	PDI	1.6	1.4
	ME (kDa)	1331.2Aa	469.4Ab

639

640

Figures

Fig. 1: Schematic diagrams of the structural models for pectin assembly. (A). Classical model depicting the pectin backbone as an extended chain with HG (smooth) and RGI (hairy) regions (De Vries et al., 1982). (B). An alternative model showing pectin formed by a RGI backbone containing neutral polymers, HG and XGA side chains (Vincken et al., 2003). (C). Model proposed by Yapo (2011) in which the pectin complex is formed by a RGI core connected with two unbranched HG blocks at the extremes. Neutral polymers, XGA and other HG blocks are side chains of the RGI core. (D). Hypothetical strawberry pectin structure deduced from the results obtained in this research. Linear pectin chains observed by AFM would be a mixture of HG chains and complex molecules formed by a HG domain of about 110 residues linked to a RGI core (52 residues). The HG unit is unbranched or contains a few number of HG branches. RGII could be linked to the HG unit allowing the formation of pectin aggregates through borate diester bridges between adjacent RGII from different pectic molecules. dp: degree of polymerization.

Fig. 2: Representative topographical AFM images of sodium carbonate soluble pectins from cell wall extracts of ripe control fruits incubated with endo-PG at different time intervals. Arrows indicate pectin complexes. Figure contrast was automatically adjusted with the software Gwyddion for a better visualization. The scale bars correspond to 100 nm.

Fig. 3: Representation of the number average (L_N) of linear chains at different endo-PG digestion times. The curves corresponds to the adjustment of the data to an exponential decay curve using the equation $L_N = L_{N0} + a.e^{-bx}$, being L_{N0} the minimum polymer chain length, a the difference between the maximum L_N value and L_{N0}, and b a rate constant.

Fig. 4: Representative error mode (A, B) and topographical (C, D) AFM images of sodium carbonate soluble pectins from cell wall extracts of ripe APG fruits before (A, C) and after hydrolysis with 0.1M HCl for 30 min at RT (B, D). Arrows indicate pectin complexes. The scale bars correspond to 100 nm.

Supplementary material

Supplementary Table 1. Descriptors of contour length distributions of linear pectin chains and aggregates extracted from ripe APG strawberry fruits after mild hydrolysis with 0.1M HCl at room temperature for 30 min. L_N, M_N: number-average, L_W, M_W: weight-average, PDI: L_W/L_N ratio, ME: median values of the original data. ME values with different letters are significantly different by the Median test at P=0.05.

Supplementary Fig. 1: Representative topographical AFM images of sodium carbonate soluble pectins from cell wall extracts of ripe APG fruits incubated with endo-PG at different time intervals. Figure contrast was automatically adjusted with the software Gwyddion for a better visualization. The scale bars correspond to 100 nm.

Supplementary Fig. 2: Representative topographical AFM images of sodium carbonate soluble pectins from cell wall extracts of ripe APEL fruits incubated with endo-PG at different time intervals. Figure contrast was automatically adjusted with the software Gwyddion for a better visualization. The scale bars correspond to 100 nm.

Supplementary Fig. 3: Detailed images of linear chains and aggregates observed in AFM samples of strawberry pectins. (A) Branched chains before digestion with endo-PG. (B) Linear chains after 4 h of digestion with endo-PG. (C) Micellar aggregates before digestion with endo-PG showing entangled pectins in the centre with emerging chains. (D) Aspect of aggregates after digestion with endo-PG, showing a reduction in complex volume and the almost disappearance of the emerging chains.

Supplementary Fig. 4: Contour length distribution of sodium carbonate soluble polymers isolated from fruit cell walls of control, APG and APEL ripe fruits. Bars represent relative frequencies of the observed data.

Supplementary Fig. 5: Percentages of branched polymer chains after digestion with endo-PG at different time intervals.

Figure 1

Click here to download high resolution image

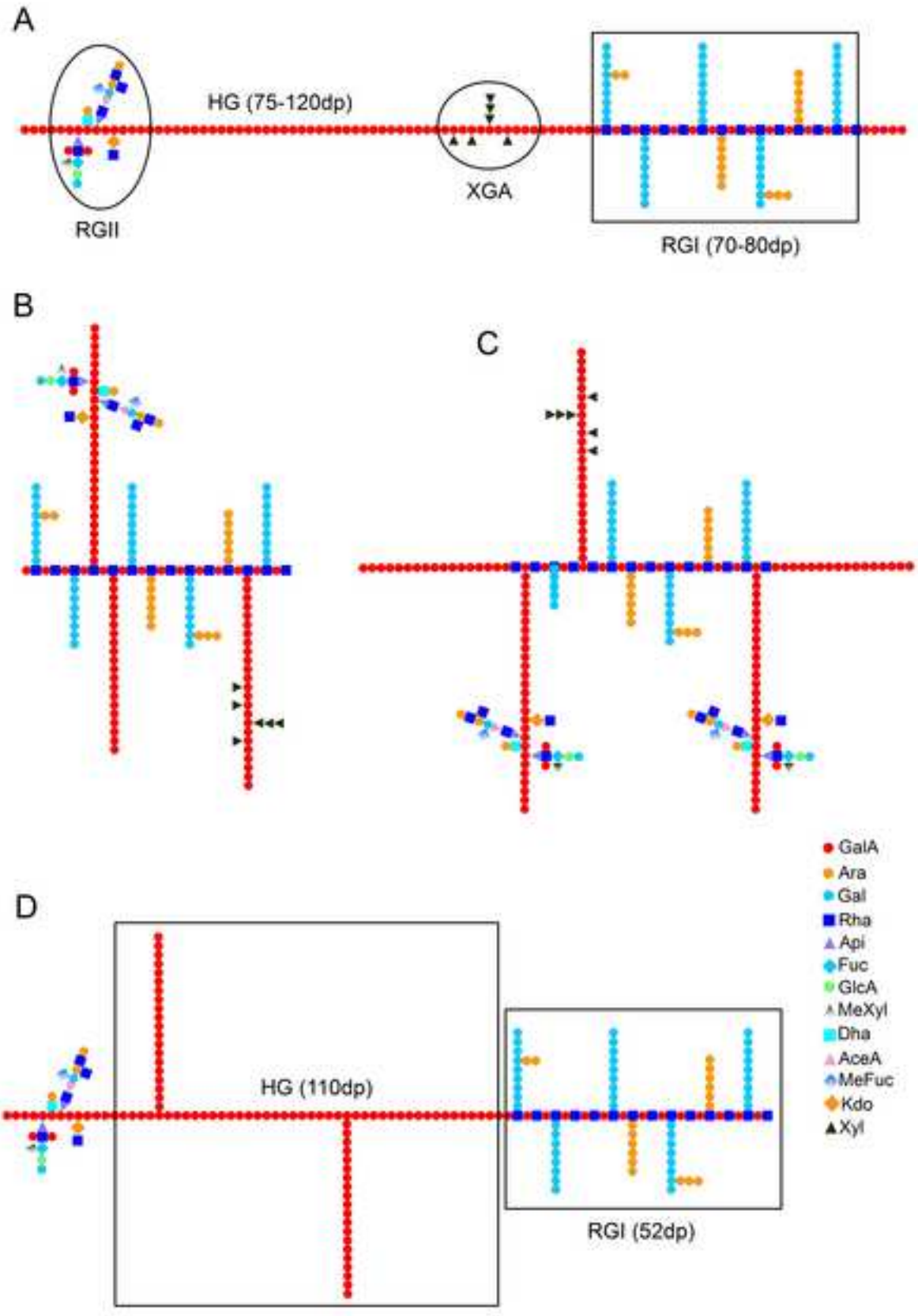

Figure 2

Click here to download Figure(s): Fig_2_New.ppt

Figure 2: Representative topographical AFM images of sodium carbonate soluble pectins from cell wall extracts of ripe control fruits incubated with endo-PG at different time intervals. Arrows indicate pectin complexes. Figure contrast was automatically adjusted with the software Gwyddion for a better visualization. The scale bars correspond to 100nm.

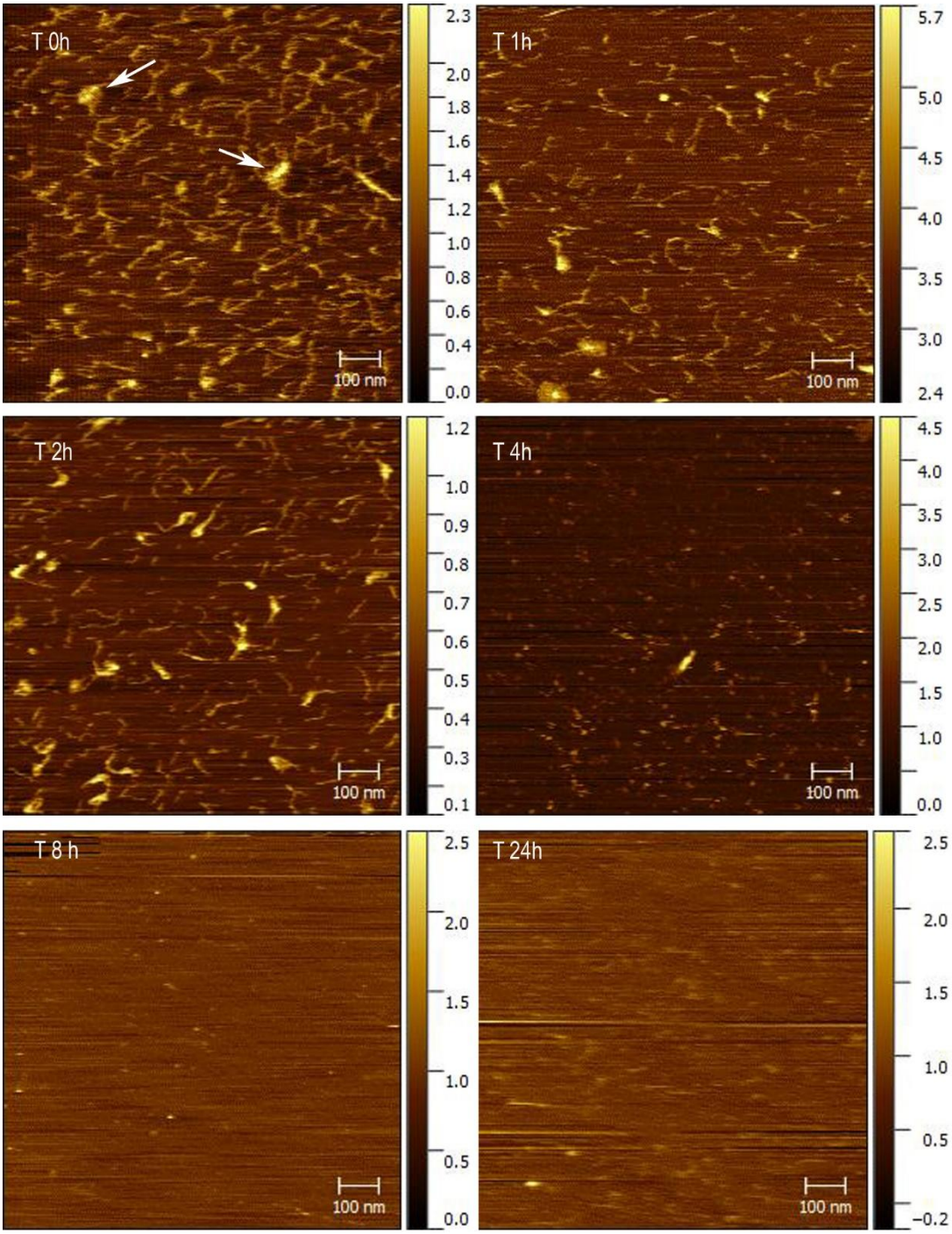

Figure 3

Click here to download Figure(s): Fig_3.ppt

Fig. 3: Representation of the number average (L_N) of linear chains at different endo-PG digestion times. The curves corresponds to the adjustment of the data to an exponential decay curve using the equation $L_N = L_{N0} + a.e^{-bx}$, being L_{N0} the minimum polymer chain length, a the difference between the maximum L_N value and L_{N0}, and b a rate constant.

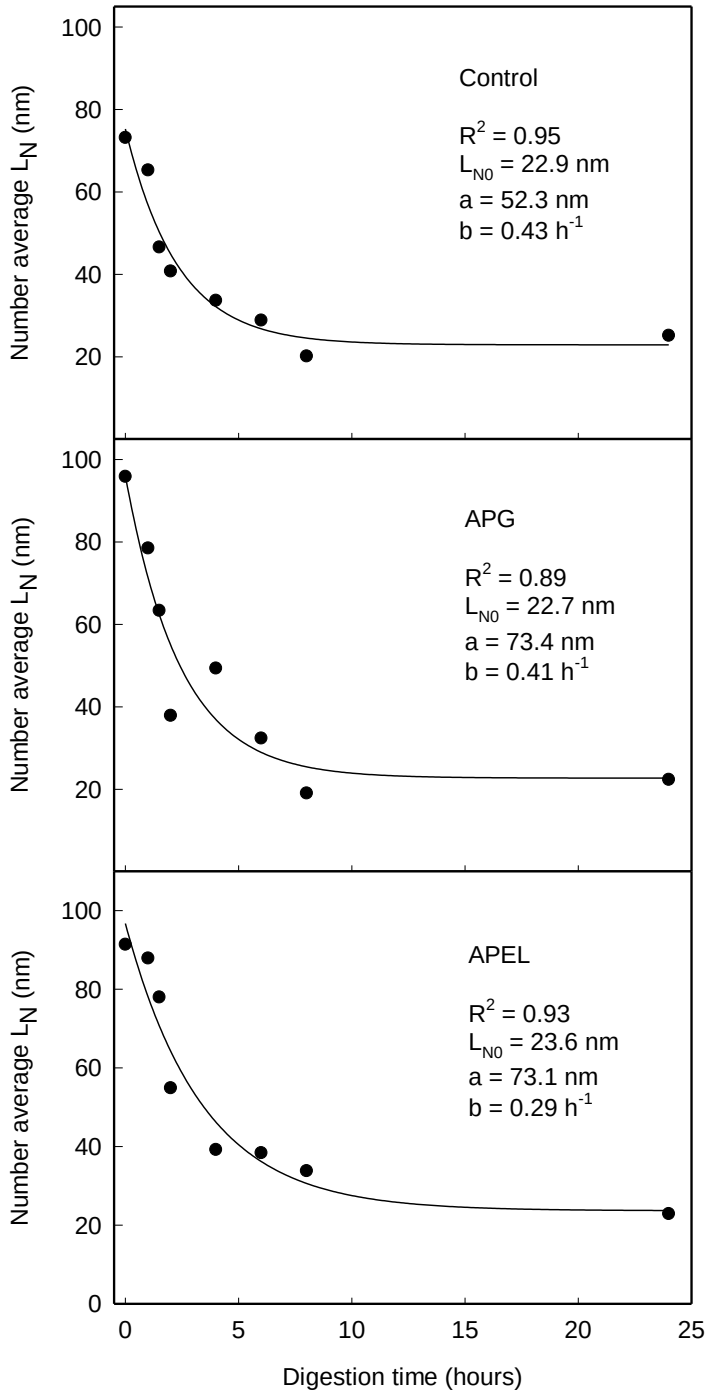

Figure 4

Click here to download Figure(s): Fig_4.ppt

Fig. 4: Representative error mode (A, B) and topographical (C, D) AFM images of sodium carbonate soluble pectins from cell wall extracts of ripe APG fruits before (A, C) and after hydrolysis with 0.1M HCl for 30min at RT (B, D). Arrows indicate pectin complexes. The scale bars correspond to 100nm.

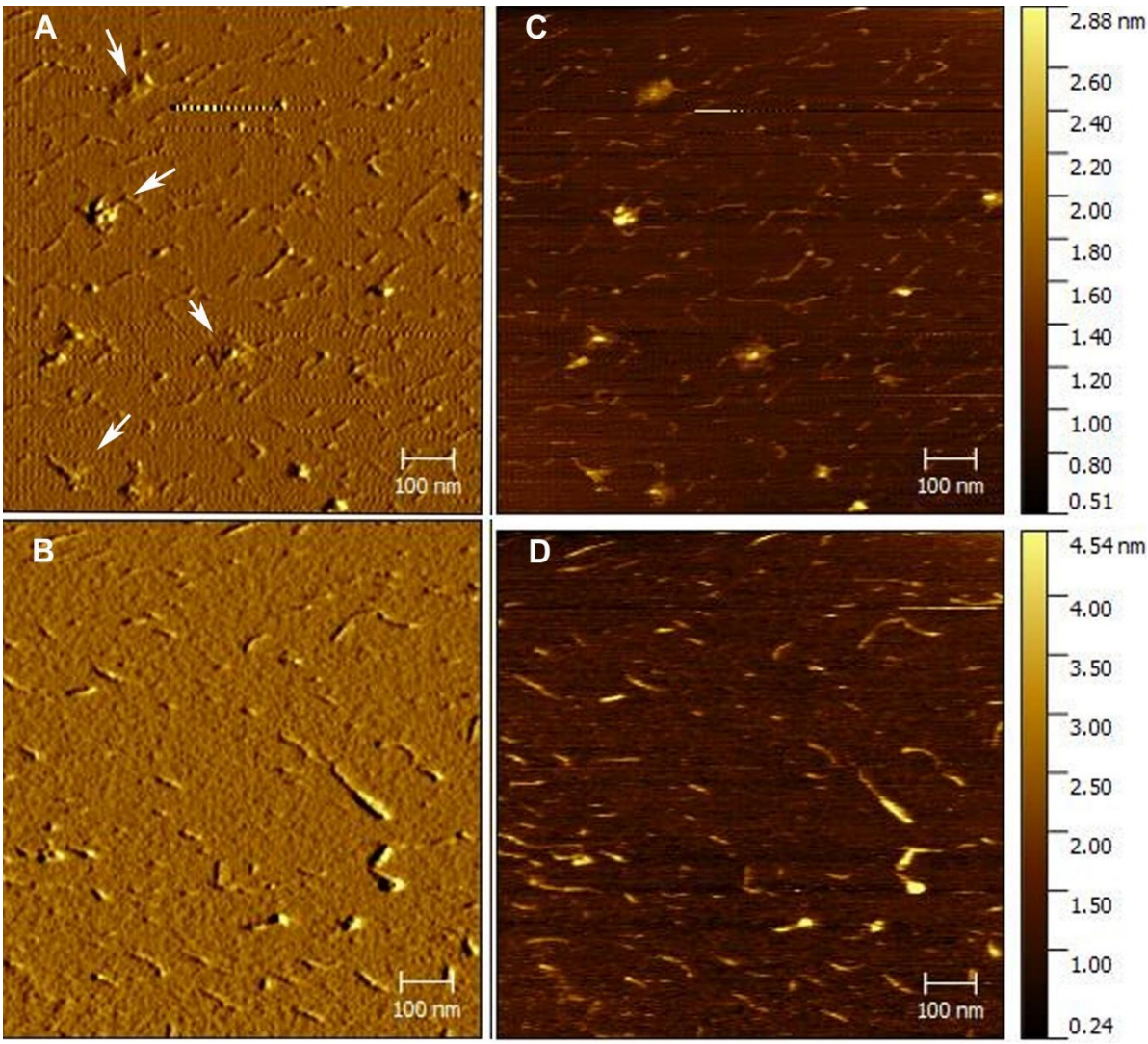

Supplementary Material

Click here to download Supplementary Material: Supplementary material-revised.pdf